DOI 10.26724/2079-8334-2026-1-95-190-198
UDC 616.833-009.17-092.9:615.277

Kulynych H.B., Herashchenko S.B., Klishch I.P., Fedorak V.M., Pertsovych V.M., Markiv I.M.
Ivano-Frankivsk National Medical University, Ivano-Frankivsk

TEMPORAL DYNAMICS OF ULTRASTRUCTURAL DAMAGE TO THE RAT SCIATIC NERVE UNDER THE EFFECTS OF CISPLATIN, PACLITAXEL, AND THEIR CONCURRENT ADMINISTRATION

e-mail: galija1979@ukr.net

Chemotherapy-induced peripheral neuropathy remains one of the most common dose-limiting complications of cisplatin- and paclitaxel-based regimens. The aim of the study was to characterize the ultrastructural changes and their temporal dynamics in the rat sciatic nerve following separate and combined administration of these agents. Adult male inbred rats were divided into four groups: intact control, paclitaxel (cumulative dose 8 mg/kg i.p.), cisplatin (cumulative dose 16 mg/kg i.p.), and a combination group. During concurrent administration, animals received cisplatin at a dose of 2 mg/kg and paclitaxel at a dose of 5 mg/kg once weekly for six weeks. The selected regimen provided a cumulative dose exposure comparable to standard clinical protocols of paclitaxel (175 mg/m²) and cisplatin (75 mg/m²) when converted on the basis of body surface area. Sciatic nerve specimens were examined by transmission electron microscopy on days 1, 7, 60, 90, and 120 after treatment initiation, with morphometric assessment of endoneurial capillary basal lamina thickness. Cisplatin induced early and pronounced endothelial-vascular damage (basal lamina thickening up to 255±30 nm, increased micropinocytosis, blood stasis, and perivascular oedema). Paclitaxel predominantly affected the axon-glial unit, causing periaxonal vacuolization, early myelin splitting, and mitochondrial degeneration in Schwann cells. Concurrent administration produced synergistic destruction of all neuro-glio-vascular components, with the most severe basal lamina thickening (280±33 nm at day 90), total myelin disorganization, massive axonal loss, and endoneurial fibrosis. By day 120, only partial recovery was observed, with persistent basal lamina thickening and chronic axonal atrophy. The results demonstrate that endothelial dysfunction and impairment of the blood-nerve barrier represent the earliest and leading events in the CIPN cascade. These findings provide morphological evidence for the development of early neuroprotective strategies focused on stabilization of the blood-nerve barrier and mitochondrial homeostasis in patients receiving cisplatin- and paclitaxel-containing chemotherapy.

Key words: chemotherapy-induced peripheral neuropathy, cisplatin, paclitaxel, sciatic nerve, ultrastructure, blood-nerve barrier, transmission electron microscopy.

Кулинич Г.Б., Геращенко С.Б., Кліщ І.П., Федорак В.М., Перцович В.М. , Марків І.М.

ЧАСОВА ДИНАМІКА УЛЬТРАСТРУКТУРНИХ УШКОДЖЕНЬ СІДНИЧНОГО НЕРВА ЩУРІВ ЗА УМОВ ДІЇ ЦИСПЛАТИНУ, ПАКЛІТАКСЕЛУ ТА ЇХ ОДНОЧАСНОГО ВВЕДЕННЯ

Хіміотерапевтично-індукована периферична нейропатія є одним із найпоширеніших дозолімітуючих ускладнень при застосуванні цисплатину та паклітакселу. Метою дослідження було охарактеризувати ультраструктурні зміни сідничного нерва щурів та їхню часову динаміку при окремому та комбінованому введенні цих препаратів. Дослідження виконано на статевозрілих самцях білих інбредних щурів, розподілених на чотири групи: інтактний контроль, паклітаксел (сумарно 8 мг/кг в/о), цисплатин (сумарно 16 мг/кг в/о) та група одночасного введення. При одночасному введенні тварини отримували цисплатин у дозі 2 мг/кг та паклітаксел у дозі 5 мг/кг один раз на тиждень протягом шести тижнів. Обрана схема забезпечувала кумулятивне дозове навантаження, співмірне зі стандартними клінічними режимами паклітакселу 175 мг/м² і цисплатину 75 мг/м² при перерахунку за площею поверхні тіла. Ультраструктуру нерва вивчали методом трансмісійної електронної мікроскопії на 1, 7, 60, 90 та 120 добу після початку введення препаратів із морфометричним визначенням товщини базальної мембрани ендоневральних капілярів. Цисплатин викликав ранні та виражені ендотеліосудинні ушкодження (потовщення базальної мембрани до 255±30 нм, мікропіноцитоз, стаз, периваскулярний набряк). Паклітаксел переважно уражував аксонально-гліальну ланку (периаксональні вакуолі, розшарування мієліну, мітохондріальна дегенерація у шванівських клітинах). Одночасне введення спричиняло синергічну деструкцію всіх компонентів нейро-гліо-судинного комплексу з максимальною товщиною базальної мембрани 280±33 нм на 90-ту добу. На 120-ту добу відзначали лише часткове відновлення з ознаками хронічної аксональної атрофії та стійкого потовщення базальної мембрани. Встановлено, що саме порушення роботи ендотелію запускає й визначає подальший розвиток ушкоджень при хіміотерапевтично-індукованій периферичній нейропатії. Отримані дані обґрунтовують необхідність ранніх нейропротекторних стратегій, спрямованих на стабілізацію гемато-нервового бар'єра та мітохондріального гомеостазу.

Ключові слова: хіміотерапевтично-індукована периферична нейропатія, цисплатин, паклітаксел, сідничний нерв, ультраструктура, електронна мікроскопія.

Funding. *The study is a fragment of the research project "Pathophysiological and morphofunctional changes of organs and systems under the influence of antitumor drugs and methods of their correction", state registration No. 0125U004275.*

Chemotherapy-induced peripheral neuropathy (CIPN) remains one of the most common and clinically significant complications of modern anticancer treatment. The development of neurotoxic lesions of the peripheral nervous system often becomes the main reason for dose reduction or early discontinuation of chemotherapy, which directly affects the efficacy of oncological treatment and patient prognosis [2, 10, 15]. Platinum agents and taxanes, particularly cisplatin and paclitaxel, which are widely used in standard treatment regimens for solid tumors, demonstrate the most pronounced neurotoxicity [2, 12, 15].

The clinical presentation of CIPN includes paresthesia, dysesthesia, allodynia, neuropathic pain,

and disturbances in gait and fine motor skills, which significantly impair patients' quality of life and often persist for a long time after treatment completion [2, 12, 15]. Despite the similarity of clinical manifestations, the morphological mechanisms of peripheral nerve damage differ significantly depending on the cytostatic drug used.

Cisplatin is characterized by predominant damage to the microvasculature with the development of endothelial dysfunction, thickening and structural disorganization of the basement membrane, disruption of the blood–nerve barrier, and the formation of chronic hypoxia of nerve fibers. The vascular component is considered one of the early and pathogenetically significant links in platinum-induced neurotoxicity, leading to subsequent axonal degeneration and demyelination [2, 10, 15].

In contrast, paclitaxel exerts a predominantly direct axonotoxic effect associated with impaired axonal transport due to microtubule hyperstabilization. This is accompanied by early damage to Schwann cells, vacuolization of the periaxonal space, destruction of myelin sheaths, and pronounced mitochondrial dysfunction, especially in sensory axons [3, 5, 8, 9]. Mitochondrial damage and oxidative stress are regarded as common key mechanisms that sustain the progression of neuropathy and limit the reparative capabilities of the peripheral nerve [3, 5].

The combined use of cisplatin and paclitaxel, which is widely used in clinical practice, is associated with a more severe and accelerated development of neurotoxic changes. Under conditions of simultaneous action, there is a synchronous involvement of the vascular, glial, and axonal-myelin components of the nerve trunk, which goes beyond a simple dose-dependent effect and indicates an interconnected amplification of various pathogenetic links of damage [2, 10, 12, 15].

This limits the understanding of the sequence of pathogenetic events and complicates the rationale for early neuroprotective strategies [2, 15].

Despite a significant number of experimental and clinical studies, most works focus on functional or behavioral manifestations of CIPN, while detailed ultrastructural characterization of peripheral nerve changes, especially regarding their dynamics and under conditions of combined chemotherapy, remains insufficiently studied.

The purpose of the study was to characterize ultrastructural changes in the sciatic nerve of rats on days 1, 7, 60, 90, and 120 following the administration of paclitaxel, cisplatin, and their combination, in order to clarify the developmental sequence of chemotherapy-induced peripheral neuropathy.

Materials and methods. The study was conducted on 120 adult male white inbred rats weighing 180–220 g. The study was carried out between April and October 2025. The experimental phase began on April 2, 2025 and continued until the completion of the maximum observation period of 120 days. Only male rats were used to avoid hormonal variability associated with the estrous cycle in females, which may influence neurotoxicity and morphometric parameters of peripheral nerves. The animals were distributed into four experimental groups:

– Group 1 (Control): animals received equivalent volumes of sterile physiological saline (0.9 % NaCl) administered intraperitoneally or intravenously according to the same schedule as the corresponding experimental groups.

– Group 2 (Paclitaxel): paclitaxel (Actavis, Romania–Iceland) was administered intraperitoneally at a dose of 2 mg/kg on days 0, 2, 4, and 6 (cumulative dose 8 mg/kg), according to the classical experimental model of paclitaxel-induced peripheral neuropathy described by Polomano et al. (2001).

– Group 3 (Cisplatin): cisplatin (Pfizer, USA) 2 mg/kg intraperitoneally, twice weekly for 4 weeks (cumulative dose 16 mg/kg), according to established experimental models of cisplatin-induced peripheral neuropathy (Carozzi et al., 2015).

– Group 4 (Concurrent): simultaneous administration of cisplatin (Pfizer, USA) at a dose of 2 mg/kg intraperitoneally and paclitaxel (Actavis, Romania–Iceland) at a dose of 5 mg/kg intravenously once weekly for six administrations. The selected regimen is dose-equivalent to the clinical chemotherapy protocol widely used in the treatment of ovarian cancer (paclitaxel 175 mg/m² combined with cisplatin 75 mg/m², 6 cycles) according to NCCN Clinical Practice Guidelines in Oncology (USA, 2024), recalculated for rats based on body surface area [11].

Each group consisted of 30 animals. Rats were housed in the vivarium of Ivano-Frankivsk National Medical University under standard conditions (temperature 21±2 °C, relative humidity 55–60 %, 12/12 h light–dark cycle) with ad libitum access to food and water.

Animals were kept in polycarbonate cages (40 × 25 × 20 cm) with stainless-steel wire lids, five animals per cage. Wood shavings were used as bedding material and were replaced regularly to maintain hygienic conditions. Environmental enrichment was provided using paper nesting material and wooden gnawing sticks to allow natural exploratory and gnawing behavior.

The adaptation period was 7 days. Euthanasia was performed by inhalation overdose of ether anesthesia. No mortality was observed throughout the experiment. Drug administration commenced on April 2, 2025. Sciatic nerve samples were collected on days 1, 7, 60, 90, and 120 from the start of chemotherapy, allowing for the assessment of the acute, subacute, and long-term phases of chemotherapy-induced peripheral neuropathy development.

To model neurotoxicity under simultaneous cytostatic administration, doses were selected to correspond to those clinically used in the treatment of ovarian, lung, and breast cancer, calculated based on rat body surface area [11].

Sample Preparation and Microscopy. Material collection for electron microscopy was performed on days 1, 7, 60, 90, and 120 after the start of drug administration. Fragments of the lumbosacral spinal cord, dorsal root ganglia, and sciatic nerve segments (~1 mm³) were harvested. For the electron microscopic study presented in this publication, sciatic nerve fragments (~1 mm³) were selected. The lumbosacral spinal cord and dorsal root ganglia were simultaneously collected for subsequent stages of the comprehensive study; however, these results are not addressed in this article.

Fixation was performed by immersion in 2 % osmium tetroxide in 0.1 M phosphate buffer (pH 7.4) for 2 hours, followed by three washes in buffer of the same molarity for 30 minutes each. Dehydration was carried out in an ascending ethanol series: 50 %, 70 %, 90 %, and 100 %. After preliminary contrasting with uranyl acetate, samples were transferred to acetone and gradually impregnated with a mixture of acetone and Epon 812/Araldite epoxy resins in ratios of 3:1, 1:1, and 1:3. Final embedding was performed with standard polymerization at 56°C for 24 hours.

Ultrathin sections were obtained using a UMTP-2M ultramicrotome, mounted on 1 mm diameter copper grids, and stained with uranyl acetate and lead citrate. Ultrastructural analysis was conducted using a PEM-125K transmission electron microscope at magnifications of ×4800–×16000.

Morphometric Analysis and Statistics. Morphometric assessment was performed on digital micrographs of semi-thin transverse sections of the sciatic nerve obtained via light microscopy (×40 objective). The area and perimeter of transverse profiles of myelinated nerve fibers (MNF) and their axons were determined interactively using UTHSCSA Image Tool® for Windows® (version 2.00) software. The analyzer was calibrated using a “MIRA” test object (GK 7.216.028-01, Research Institute “Kvant”).

Based on the primary data, the myelin sheath cross-sectional area, form factors of MNFs and axons, and the g-ratio (gS) were calculated. Statistical analysis was performed using GraphPad Prism 9.0 and Statistica 6.0 for Windows. The normality of distribution was verified using the Kolmogorov–Smirnov/Lilliefors and Shapiro–Wilk tests. Intergroup comparisons were made using one-way analysis of variance (ANOVA) with Tukey’s post-hoc test. Differences were considered statistically significant at $p<0.05$. For each group and time point, 40–50 morphometric measurements obtained from 5–6 animals were analyzed.

All procedures were performed in accordance with the European Convention for the Protection of Vertebrate Animals used for Experimental and Other Scientific Purposes (Strasbourg, 1986) and the Declaration of Helsinki (2013). The study was approved by the Bioethics Committee of Ivano-Frankivsk National Medical University (Protocol No. 146/24 dated September 26, 2024). All animals survived until the completion of the experiment.

Results of the study and their discussion. The ultrastructural organization of the sciatic nerve was analyzed in intact animals and in rats subjected to different chemotherapy regimens. Particular attention was paid to the structural state of myelinated and unmyelinated nerve fibers, Schwann cells, and endoneurial components, which are known to be sensitive indicators of chemotherapy-induced neurotoxicity. These observations served as the basis for subsequent comparative analysis of the experimental groups.

Prior to analyzing the experimental groups, the ultrastructure of the sciatic nerve of the intact rat was examined to determine the normal morphological organization. In intact animals, an ordered structure of both unmyelinated and myelinated nerve fibers (MNF) was preserved, serving as a baseline for comparison (Fig. 1).

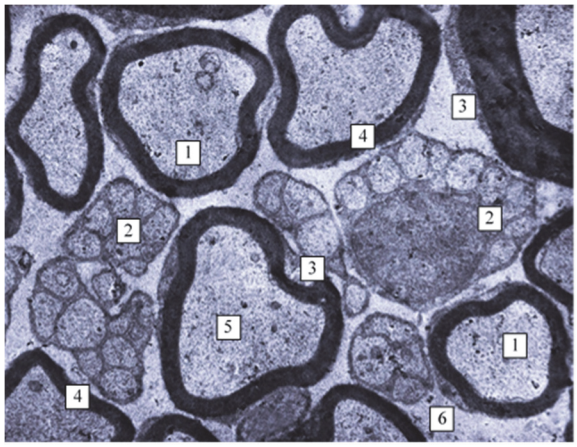

Fig. 1. Ultrastructure of the rat sciatic nerve (intact group). 1 – myelinated nerve fibers, 2 – unmyelinated nerve fibers, 3 – Schwann cell cytoplasm, 4 – myelin sheath, 5 – axoplasm, 6 – endoneurium. Electron micrograph. Magnification: ×4800.

In animals of the intact group, the sciatic nerve ultrastructure corresponded to the physiological norm. MNFs possessed a regular shape without signs of destruction. Axons featured evenly distributed neurofilaments and mitochondria. Unmyelinated fibers were arranged in Remak bundles. The interfibrillar space was not dilated, and signs of edema or collagenization were absent. Microvessels of the epi- and perineurium possessed a thin, continuous basement membrane.

Electron micrographs present a fragment of the rat sciatic nerve endoneurium, where Remak bundles predominate, showing several unmyelinated axonal profiles within the Schwann cell cytoplasm and solitary MNFs (Fig. 2).

On day 1 post-paclitaxel administration, early but distinct signs of toxic damage to unmyelinated

fibers were evident in the endoneurium. Characteristic Remak bundles were identified, in which small axons lay within the Schwann cell cytoplasm. This represents an early reaction to the disruption of microtubular transport caused by paclitaxel.

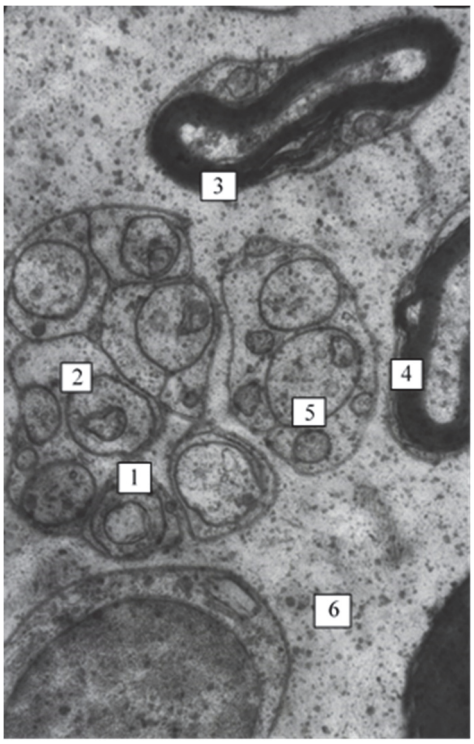

A

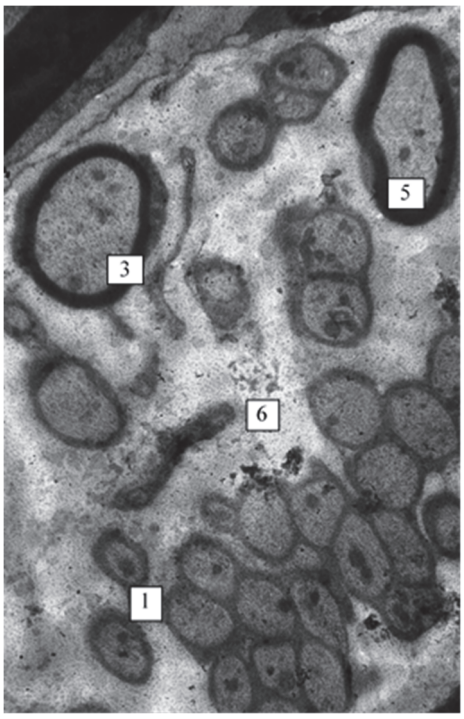

B

Fig. 2. Ultrastructure of the rat sciatic nerve – paclitaxel group (a – day 1 after paclitaxel administration, b – day 7 after paclitaxel administration). 1 – unmyelinated nerve fibers, 2 – Schwann cell cytoplasm, 3 – myelinated nerve fiber, 4 – local protrusion of myelin lamellae, 5 – axoplasm, 6 – endoneurium. Electron micrographs. Magnification: a – ×3200, b – ×4800.

Centrally, a structure with homogeneous electron density was observed a transverse section of a large unmyelinated axon that maintained an intact plasmalemma and showed no signs of acute destruction. The Schwann cell cytoplasm appeared locally condensed with solitary osmiophilic granules, indicating an early endoplasmic stress response. The Schwann cell plasmalemma was uniform without significant detachment, corresponding to an initial level of injury. The perineural interstitium was moderately edematous without massive disorganization. Axons were rounded with smooth contours, and the axoplasm was fine-grained and homogeneous. In the lower portion, a large myelinated axon with preserved lamellar myelin structure was visible: plates were densely arranged without ruptures, interlamellar clefts, or areas of loosening. The interfibrillar space was homogeneous, lacking osmiophilic inclusions, indicating a normal state of the endoneurial matrix. On the right, a transverse profile of a capillary with a uniform basement membrane and thin endothelium was visible.

This combination of minimal axonal changes, moderate edema, and Schwann cell reactivity corresponded to the early phase of paclitaxel-induced neurotoxicity, where structural disturbances were only beginning to form but had not yet progressed to pronounced demyelination or axonal disintegration mediated by inflammatory factors.

MNFs showed signs of early demyelination: indistinct lamellar contours, formation of interlamellar vacuoles, and areas of loosening. The axoplasm of individual axons lost its homogeneity and contained foci of fragmentation. Small osmiophilic inclusions and moderate edema were identified in the interfibrillar space.

On day 7 after paclitaxel administration, moderate dystrophic changes were observed without massive destruction. Myelin sheaths in some fibers were locally delaminated, and vacuolization, reduced electron density, and initial periaxonal edema were determined in individual axons. Small vesicles and solitary areas of mitochondrial outer membrane destruction were found in the Schwann cell cytoplasm. The arrangement of Remak bundles was preserved; however, individual unmyelinated axons exhibited a wavy contour configuration and signs of early swelling. The interfibrillar space was moderately dilated with an increased amount of electron-light amorphous material. Perineural cells occasionally contained large vacuoles, reflecting the activation of autophagic processes. Vessels of the microvasculature retained their structure, and the perineurium remained intact.

By day 60, chronic changes were still observed: intensified axon vacuolization, partial demyelination with the formation of concentric myelin figures, and mitochondrial degeneration with loss of cristae. Schwann cells exhibited hyperplasia, and perivascular edema persisted.

By day 90, changes acquired a persistent character: axonal atrophy, basement membrane

fibrosis, and reduced nerve fiber density, but without acute inflammation.

On day 120 of the experiment, the ultrastructure of endoneurial hemomicrocirculatory elements returned to a habitual appearance. Only moderate luminal dilation and solitary areas of mild basement membrane edema remained. Signs of partial recovery were recorded, accompanied by remyelination of some fibers and a reduction in vacuoles; however, residual fibrotic changes in the epineurium persisted.

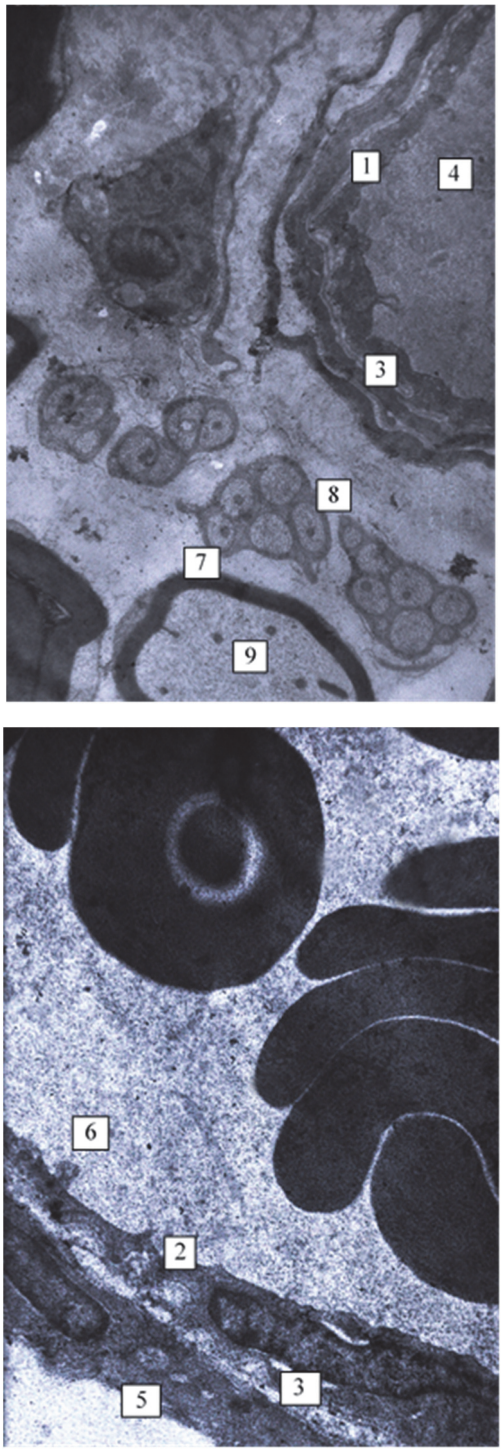

Fig. 3. Ultrastructure of the rat sciatic nerve, cisplatin group (a – day 1 after cisplatin administration; b – day 7 after administration). 1 – endothelium, 2 – vacuoles, 3 – basement membrane, 4 – postcapillary venule, 5 – pericyte, 6 – venular lumen, 7 – myelinated nerve fiber, 8 – unmyelinated nerve fiber, 9 – axon. Transmission electron micrographs. Magnification: a ×8600, b ×6400.

Thus, throughout the observation period, a general pattern of changes in the microvasculature vessels was traced. These manifested as congestion (hyperemia), signs of impaired transendothelial transport, varying degrees of endothelial cell dystrophy, and thickening and partial dissociation of the basement membrane.

In the postcapillary venules of the epineurium, a sharply increased diameter, congestion (hyperemia), and erythrocyte stasis were observed. The endothelium was thinned and contained numerous micropinocytotic vesicles, vacuoles, and transendothelial channels. The luminal plasmalemma formed solitary protrusions into the vessel lumen, while the basement membrane was sharply thickened. Deformation of pericyte processes and their vacuolization, as well as pronounced perivenular edema, were noted (Fig. 3).

On day 1 of cisplatin exposure, microvessels of the perineurium exhibited a thickened basement membrane, partial endothelial proliferation, and pericapillary edema. Schwann cells of adjacent fibers were vacuolated with local areas of destruction. The picture corresponded to a compensatory-inflammatory reaction typical of the acute phase of neurotoxicity. Electron micrographs of the epineurial capillary also determined uneven thickening of the endothelium with solitary protrusions of the luminal surface, focal dissociation of the basement membrane, and an increase in the number of micropinocytotic vesicles located on the luminal and adluminal plasmalemma. In the surrounding areas, there was moderate edema of unmyelinated fibers with preservation of pericyte-endothelial contacts. These changes indicated an acute disruption of the barrier function of microvessels at the early stage of cisplatin-induced neurotoxicity.

On day 7, a zone of early destructive changes in myelinated nerve fibers (MNF) formed. Axons lost homogeneity, and the axoplasm was fragmented with electron-light cavities. Myelin lamellae ruptured and formed concentric structures. The cytoplasm of Schwann cells was in a state of disintegration, containing osmiophilic granules-signs of the early phase of neurodegeneration. Minor changes were observed in small-diameter MNFs the structure was predominantly preserved; however, in medium fibers, interlamellar vacuoles and delamination of the inner and outer myelin layers were detected.

On day 60 of observation, severe axonal degeneration, practically total loss of myelin sheaths, and marked mitochondrial collapse accompanied by the accumulation of electron-dense osmiophilic inclusions were noted. At the same time, significant interstitial fibrosis of the endoneurium with thickening of collagen fibers and narrowing of the microvascular lumen was observed.

By day 90, the process acquired a chronic course: atrophy of nerve fibers of various calibers dominated, persistent tissue edema remained, and

marked proliferation was detected among Schwann cells with the formation of so-called "onion bulb" structures and signs of fibrous reorganization. Regenerative activity at this stage remained minimal.

On day 120, the first signs of partial remyelinating recovery appeared, predominantly in small-caliber fibers; newly formed myelin had a lamellar organization but was thinner than normal. Despite this, most axons retained signs of residual atrophy, and the endothelium of microvessels and basement membranes of Schwann cells remained thickened, indicating the incompleteness of reparative processes and the persistence of the structural basis for chronic neuropathy.

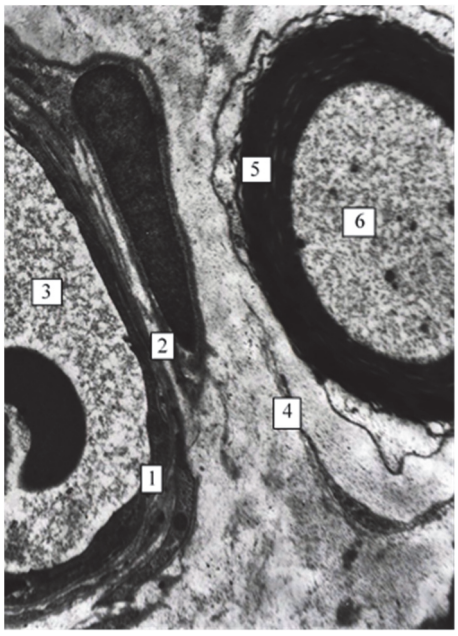

A

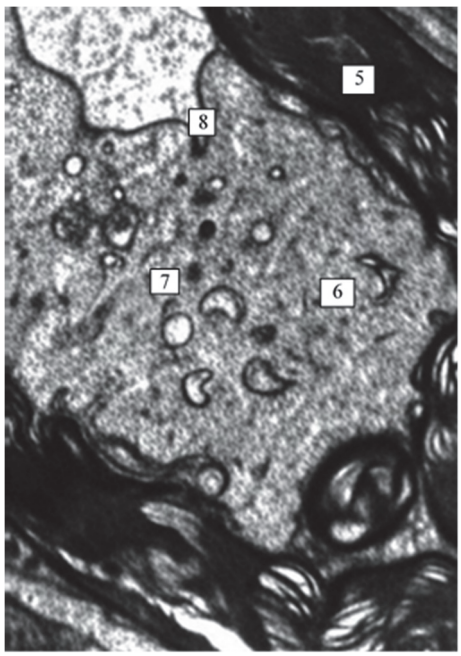

B

Fig. 4. Ultrastructure of the sciatic nerve concurrent Cisplatin and Paclitaxel Group (a – 1st day after simultaneous administration, b – 7th day after simultaneous administration). 1 – endothelial cell, 2 – basement membrane, 3 – venule lumen, 4 – fibroblast, 5 – myelin sheath, 6 – axial cylinder, 7 – mitochondria, 8 – vacuole. Electron micrographs. Magnification: a – ×4800, b – ×6400.

Pronounced degenerative-destructive changes were revealed. Myelin sheaths underwent total disorganization; in many fibers, concentric "myelin figures" formed. Large-diameter MNFs of varying thickness were determined. Significant disturbances in the orientation of myelin sheath lamellae and the formation of interlamellar vacuoles filled with homogeneous structureless masses were noted. The thickness of axial cylinders was sharply reduced, with deformation of axial cylinders and the formation of protrusions within the thickness of the myelin sheath. Alongside solitary destroyed mitochondria, numerous profiles of neurotubules and neurofilaments were determined. In small-diameter MNFs, the structure of the myelin sheath was generally preserved, but in some, the myelin sheath formed protrusions, which occasionally appeared as intra-axonal myelin fragments with predominantly circular or chaotic lamellar orientation.

In the postcapillary venules of the epineurium, a sharply increased diameter, congestion, and erythrocyte stasis were observed. The endothelium was thinned, containing numerous micropinocytotic vesicles, vacuoles, and transendothelial channels. The luminal plasmalemma formed solitary protrusions into the vessel lumen, and the basement membrane was sharply thickened. Deformation of pericyte processes and their vacuolization, as well as pronounced perivenular edema, were noted (Fig. 4).

On day 1 after simultaneous administration of cisplatin and paclitaxel, venules of sharply increased diameter and congestion (in the epineurium) were revealed. The endothelium was thinned, with numerous micropinocytotic vesicles and small vacuoles that merged to form transendothelial channels. The luminal plasmalemma formed solitary finger-like protrusions into the vessel lumen. The adluminal surface of endothelial cells, conversely, was extremely active, forming protrusions, “veils” and “sails” penetrating the thickness of the basement membrane, which was sharply thickened. Pericytes showed dystrophy: their processes were thinned and vacuolated, and the perivenular space was edematous.

On day 7 after combined administration, pronounced degenerative-destructive changes were already evident. Myelin sheaths underwent total disorganization, and concentric “myelin figures” formed in the fibers. MNFs of various diameters with uneven sheath thickness, significant disturbances in lamellar orientation, and the formation of interlamellar vacuoles filled with homogeneous structureless masses were defined. The thickness of axial cylinders was sharply reduced; occasionally, their protrusions within the myelin sheath and shrinkage were observed. Solitary destroyed mitochondria were present in the cytoplasm. Such changes indicate the cumulative effect of both drugs on axonal transport and myelinogenesis.

Under simultaneous administration of cisplatin and paclitaxel, peripheral nerve damage proved to be significantly more severe and rapid than with monotherapy of either drug.

On day 60, massive axonal death was observed (many fibers simply disappeared), along with total fibrosis of the endoneurium and perineurium, pronounced persistent edema, and sharp proliferation of Schwann cells and other glial elements.

By day 90, the process transitioned into a chronic phase: nerve fibers were sharply thinned, their density dropped, myelin was fragmented and delaminated, and numerous electron-dense osmiophilic inclusions accumulated in the cytoplasm of Schwann cells and residual axons, indicating signs of prolonged oxidative stress.

Only on day 120 did separate signs of regeneration appear. New formation of thin myelin began in small-caliber fibers, and foci of regeneration were occasionally encountered. However, large myelinated axons remained atrophied or did not recover at all, fibrous tissue persisted, and vessel walls and basement membranes remained thickened. Thus, even after 4 months, the nerve remained structurally altered and functionally weakened.

This described sequence is characteristic specifically for the combination of platinum with taxanes and significantly exceeds the severity of isolated administration of each drug separately.

Thus, comparative analysis revealed that paclitaxel predominantly affects axonal structures and Schwann cells, whereas cisplatin exerts a pronounced vascular-endothelial effect. Simultaneous administration has a cumulative and mutually potentiating effect, leading to the destruction of all elements of the neuro-glio-vascular complex.

Morphometric analysis quantitatively confirmed the results of qualitative observations. In all experimental groups, a significant increase in the thickness of the basement membrane of epineurial capillaries was detected, indicating the development of microvascular dysfunction. The most pronounced thickening was observed in the group with simultaneous drug administration (Table 1).

Table 1

Thickness of the basement membrane of capillaries in the rat sciatic nerve epineurium (M±SD, nm)

Group	Day 1 (nm)	Day 7 (nm)	Day 60 (nm)	Day 90 (nm)	Day 120 (nm)
Intact	112±14	112±14	112±14	112±14	112±14
Paclitaxel	145±18*	162±20*	185±22*	210±25**	195±23*
Cisplatin	165±21*	188±23**	225±27**	255±30**	230±28**
Concurrent	180±23**	205±26**	245±29**	280±33**	250±30**

Notes: *p<0.05; **p<0.01 compared to the intact control for the corresponding observation period (one-way ANOVA with Tukey's post-hoc test); n = 40–50 measurements per group and time point (from 5–6 animals).

In rats of the intact group, capillary basement membrane thickness remained stable throughout the experiment at 112±14 nm. In all experimental groups, significant thickening of the basement membrane was noted as early as day 1. It progressed until day 90 and regressed by day 120. The most pronounced changes were observed in the group with combined cisplatin and paclitaxel administration (up to 280±33 nm on day 90). This confirms the synergistic character of endothelial dysfunction.

The conducted ultrastructural and morphometric study demonstrated that cisplatin and paclitaxel form damage models of the sciatic nerve that differ in mechanisms and temporal profiles. In both cases, the lesion unfolds as a sequential cascade of changes in the neuro-glio-vascular complex, yet the key pathogenetic links differ: early microvascular disturbances are typical for cisplatin, whereas axonal-glial and mitochondrial damage mechanisms predominate for paclitaxel. These changes generally correspond to modern clinical-experimental concepts of CIPN and its phasic nature [7, 8, 15].

In the cisplatin group, vascular-endothelial disorders dominated as early as day 1: thickening and heterogeneity of the capillary basement membrane, activation of micropinocytosis, stasis in postcapillary venules, and perivascular edema. These signs align well with review data where disruption of the blood–nerve barrier and microcirculation is considered an early and persistent link in platinum-induced neurotoxicity with subsequent chronification of the process [7, 8]. The progressive basement membrane thickening revealed in our study in the long term explains the prolonged disruption of metabolic processes in the nerve and the formation of conditions for axonal degeneration and demyelination, which are described as typical for established CIPN [11, 15].

Conversely, in the paclitaxel group, changes in the axonal-glial link predominated in the early stages (days 1–7): periaxonal vacuolization, initial delamination of myelin lamellae, edema, and structural remodeling of mitochondria in Schwann cells. Such a spectrum of changes corresponds to current understandings of taxane neuropathy mechanisms, where key factors are disruptions of axonal transport and energy supply with subsequent mitochondrial damage [5, 12]. Particularly indicative are data regarding mitochondrial anomalies in sensory axons during paclitaxel-induced neuropathy with pain syndrome, which reproduce the ultrastructural changes observed in our study [5]. Importantly, the mitochondrial component of toxicity and oxidative stress imbalance are regarded as leading causes for symptom persistence and limited repair [5, 15].

Special attention in pathogenesis is drawn to the glial component of damage, the significance of which is clearly traced via transmission electron microscopy data. Schwann cell edema, organelle changes, and disruption of contact with the axon are crucial in damage development. Conversely, neuro-glial interactions may sustain prolonged inflammation and nerve tissue remodeling, as summarized in studies on glial–neuronal mechanisms of CIPN [3, 4]. In this context, our observations of early Schwann cell changes logically explain why, even after the attenuation of acute manifestations, some fibers retain metabolic fragility and susceptibility to degeneration.

The most pronounced and rapidly progressing changes formed under conditions of simultaneous cisplatin and paclitaxel administration. Here, damage encompassed all components of the neuro-glio-vascular complex synchronously: sharp basement membrane thickening, deep myelin disorganization with myelin figures, massive axon loss, and pronounced endoneurial edema with signs of fibrosis. This nature of damage cannot be explained by a simple summation of toxic effects but reflects a potentiated action, where cisplatin-induced vascular disorders create conditions for the enhanced manifestation of paclitaxel axonotoxicity. Similar multicomponent damage and the clinically-experimentally confirmed severity of combined chemotherapy regimens are noted in comprehensive reviews dedicated to CIPN [7, 8, 15].

In the long term (days 60–120), signs of partial repair appeared in all experimental groups. This manifested as remyelination of a portion of small-caliber fibers and reduced edema. At the same time, persistent basement membrane thickening and atrophy of some axons demonstrated that the process is chronic and only partially reversible, especially under platinum and combined administration regimens [7, 8]. This “incomplete reconstruction” aligns with the modern view that therapeutic approaches may reduce symptoms and individual damage mechanisms, whereas structural recovery of peripheral nerves often remains limited [7]. Practically, this explains the growing interest in strategies aimed at drug optimization and combined supportive therapy in CIPN management [10, 14].

Given the obtained morphological data, the direction of neuroprotection focused on reducing mitochondrial damage and oxidative stress appears justified. Experimental evidence on the protective effect of α-lipoic acid on mitochondrial integrity in CIPN corresponds well with our observations, where mitochondrial degradation was one of the most persistent components of nerve injury [1]. Approaches aimed at modulating glial-inflammatory and signaling pathways, including cellular technologies, also appear promising, demonstrating functional and neuroprotective efficacy in experimental models of paclitaxel-induced neuropathy [2].

It is also important that the toxic impact of chemotherapy is not limited solely to the nerve as a structure. The presence of peripheral neuropathy is accompanied by broader tissue manifestations, which is reflected in studies describing morphological changes in oral cavity organs during paclitaxel-induced neuropathy [6, 13]. Such findings emphasize the systemic nature of the neuropathic process and indicate that its clinical consequences may extend beyond purely neurological symptoms.

Thus, the established temporal sequence of morphological changes – early endothelial dysfunction, glial reaction, progressive axonal degeneration with demyelination, and incomplete repair – corresponds to modern concepts of CIPN pathogenesis. The obtained ultrastructural data provide grounds to consider endothelial stabilization, modulation of glial responses, and mitochondrial protection as three key directions for early prophylaxis and correction of neurotoxicity, especially in platinum- and taxane-containing chemotherapy regimens [1, 3, 5, 7, 8].

Limitations. The present study focused primarily on morphological and ultrastructural assessment; therefore, electrophysiological parameters of nerve conduction were not evaluated. Consequently, the relationship between structural alterations and functional manifestations of chemotherapy-induced neurotoxicity could not be directly established. Further studies integrating morphological and functional approaches are required to clarify these mechanisms.

Conclusions

Simultaneous administration of cisplatin and paclitaxel causes pronounced cumulative damage to the rat sciatic nerve with sequential involvement of microvascular, glial, and axonal-myelin components and the formation of chronic degenerative changes. Cisplatin realizes its neurotoxic effect predominantly through vascular-endothelial mechanisms with disruption of the blood-nerve barrier, whereas paclitaxel primarily affects the axonal-glial link; their combination has a synergistic character leading to total disorganization of the neuro-glio-vascular complex. Morphometric data confirm the leading role of endothelial dysfunction in the pathogenesis of chemotherapy-induced peripheral neuropathy, manifested by persistent thickening of the basement membrane of peripheral nerve microvessels. The obtained results justify the expediency of early neuroprotective approaches aimed at stabilizing the vascular endothelium and supporting mitochondrial homeostasis as a promising direction for preventing and reducing the severity of chemotherapy-induced peripheral neuropathy.

References

1. Al-Massri KF, Ahmed LA, El-Abhar HS. Mesenchymal stem cells therapy enhances the efficacy of pregabalin and prevents its motor impairment in paclitaxel-induced neuropathy in rats: role of Notch1 receptor and JAK/STAT signaling pathway. Behav Brain Res. 2019;360:303-11. doi:10.1016/j.bbr.2018.12.013.
2. Chen X, Gan Y, Au NPB, Ma CHE, Zhang M, Li J, et al. Current understanding of the molecular mechanisms of chemotherapy-induced peripheral neuropathy. Front Mol Neurosci. 2024;17:1345811. doi:10.3389/fnmol.2024.1345811.
3. Cirrincione AM, Pellegrini AD, Dominy JR, Benjamin ME, Utkina-Sosunova I, Lotti F, et al. Paclitaxel-induced peripheral neuropathy is caused by epidermal ROS and mitochondrial damage through conserved MMP-13 activation. Sci Rep. 2020;10:397. doi:10.1038/s41598-020-60990-8.
4. Dong N, Zhang Y, Wang Y, Liu Q, Chen J, Zhao H, et al. Innate immune mechanisms in chemotherapy-induced peripheral neuropathy. Front Pain Res. 2025;6:1642306. doi:10.3389/fpain.2025.1642306.
5. Flatters SJL, Dougherty PM, Colvin LA, Huang H, Zhang H, Onvani S, et al. Clinical and preclinical perspectives on chemotherapy-induced peripheral neuropathy. Br J Anaesth. 2017;119(4):737-49. doi:10.1093/bja/aex229.
6. Gu L, Cao S, Feng Y. Mechanisms of spinal glial activation in chemotherapy-induced peripheral neuropathy: focus on microglia and astrocytes. Ibrain. 2025. doi:10.1002/ibra.70007.
7. Kotvytska AA, Tykhonovych KV, Kryvoruchko TD, Neporada KS, Beregovyi SM. Paclitaxel-induced neuropathy induces changes in oral cavity organs of rats. Regul Mech Biosyst. 2023;14(1):102-5. doi:10.15421/022315.
8. Lee KT, Kim JH, Park SH, Kim YS, Lee SH, Kang JW, et al. Chemotherapy-induced peripheral neuropathy: mechanisms and clinical implications. Cancers (Basel). 2024;16(14):2571. doi:10.3390/cancers16142571.
9. Maiar M, Petrini A, Angelis FD, Nazio F, Marinelli S, et al. Unveiling the peripheral nerve hallmarks of chemotherapy-induced neuropathy: insights from paclitaxel treatment in a murine model. Neurobiol Pain. 2025;18:100200. doi:10.1016/j.ynpai.2025.100200.
10. Mattar M, Umutoni F, Hassan MA, Wamburu MW, Turner R, Patton JS, et al. Chemotherapy-induced peripheral neuropathy: a recent update on pathophysiology and treatment. Life (Basel). 2024;14(8):991. doi:10.3390/life14080991.
11. Reagan-Shaw S, Nihal M, Ahmad N. Dose translation from animal to human studies revisited. FASEB J. 2008;22(3):659-61. doi:10.1096/fj.07-9574LSF.
12. Tao Z, Wang X, Zhang Y, Liu H, Chen L, Li Y, et al. Emerging aspects of cancer neuroscience in chemotherapy-induced peripheral neuropathy. Front Neurosci. 2025. doi:10.3389/fnins.2025.XXXXX.
13. Tykhonovych KV, Neporada KS, Yeroshenko HA, Yeroshenko GA. Pathomorphological changes in salivary glands of rats under diabetic neuropathy and correction. Svit Med Biol. 2023;1(83):229-32. doi: 10.26724/2079-8334-2023-1-83-229-232.
14. Yamamoto S, Egashira N. Drug repositioning for the prevention and treatment of chemotherapy-induced peripheral neuropathy: a mechanism- and screening-based strategy. Front Pharmacol. 2021;11:607780. doi:10.3389/fphar.2020.607780.
15. Ye A, Butt A, Geng Y, Abdi S. Understanding discordance in systematic reviews for treating chemotherapy-induced peripheral neuropathy: a focused umbrella review. J Clin Oncol. 2024;42(16_suppl):e24111. doi:10.1200/JCO.2024.42.16_suppl.e24111.

Conflict of interest. The authors have no conflicts of interest to declare.

ORCID: Kulynych H.B. https://orcid.org/0000-0002-0233-2282, Herashchenko S.B. https://orcid.org/0000-0003-0958-4885, Klishch I.P. https://orcid.org/0000-0001-6616-1980, Fedorak V.M. https://orcid.org/0000-0003-4607-0496, Pertsovych V.M. https://orcid.org/0000-0002-9491-6292, Markiv I.M. https://orcid.org/0009-0000-2517-6086.

Article received: 12.02.2025.